

Soot Volume Fraction Characterizations Using the Laser-Induced Incandescence Detection Method

David R. Snelling, Gregory J. Smallwood, and Ömer L. Gülder

National Research Council Canada
ICPET Combustion Research Group, Building M-9
1200 Montreal Road
Ottawa, Ontario K1A 0R6
Canada

William D. Bachalo* and Subramanian Sankar

Artium Technologies
14660 Saltamontes Way
Los Altos Hills, CA, 94022-2036
USA

*Corresponding author

Introduction:

There is an urgent need to decrease the total emissions from combustion systems including diesel and spark ignition (SI) reciprocating engines, power plants, and other industrial facilities. The undesirable exhaust emissions include CO₂, NO_x, SO_x, aerosol, and particulate matter. In particular, aerosols and particulate are known to produce adverse health effects and are suspected of contributing to high altitude clouds, which adversely affect the earth's climatology. Besides environmental and health concerns, there is also a strong need to control soot and other particulates in the exhaust plume because of their adverse influence on the performance of the power generation systems. In order to develop processes and techniques for limiting the emission of soot, we must first possess suitable means for reliably measuring various soot-related parameters.

Laser-induced incandescence (LII) detection and measurement is an emerging technology that promises to yield a reliable means for spatially and temporally measuring the soot volume fraction and primary soot particle size. With this approach, the soot within the laser beam path is heated rapidly using a pulsed laser source with duration typically less than 20ns. The soot is heated from the local ambient soot temperature to a temperature approximately equal to the soot vaporization temperature (approximately 4000°K). The incandescence from the soot particles is measured using collection optics and photodetectors. With appropriate calibration and analysis of the incandescence signal, information on the soot volume fraction and primary soot particle size may be obtained. Laser energy absorption by the soot particles and the subsequent cooling processes involve complex analysis of the nano-scale heat and mass transfer in time and space.

Background

Significant effort has been expended in an effort to characterize soot particulates using optical diagnostics. The primary problems are that the soot is generally composed of an aggregation of primary spheres with diameters less than about 60 nm and the complex index of refraction is not known with adequate certainty. Light scatter detection systems using near forward angle detection were argued to be relatively insensitive to the shape of the particles. Although this may be true for particles that do not have large aspect ratio, the long chain-like structures of the soot aggregates (figure 1) do not meet this criterion. The aggregates may vary in size from a few primary particles to equivalent diameters of 0.5µm. In addition, the near-forward scattering methods using single particle counting experienced problems with high soot concentrations. They do have an advantage at low concentrations where the light extinction methods become insensitive.

Because of the complex nature of the soot morphology, particle size or more accurately, the aerodynamic particle size measurements have been made using differential mobility particle sizers (DMPS). In this device, the particles are charged using an electric field and separated by size. The particles separated into classes are then

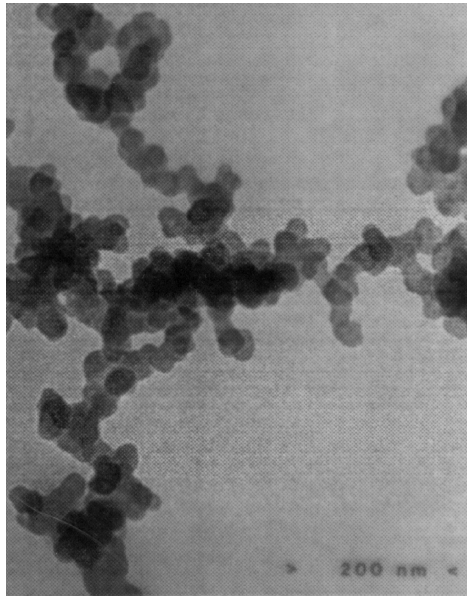


Figure 1: Soot particle micrograph from R.A. Dobbins and H. Subramaniasivam, 1994.

counted using a condensation nuclei counter (CNC) to produce a number-weighted size distribution. Another related approach for measuring particles in the size range of 0.05 to 10 μm is the electrical low-pressure impactor (ELPI). In this instrument, the particles are first charged and then passed through a cascade impactor to segregate them into bins or size classes. The current deposited on each stage of the impactor may be related to the particle concentrations in the various size classes. These methods are useful but leave a degree of uncertainty due to the sampling process and to transporting of the particle samples to the device.

A good review of the soot formation process and the nature of soot is provided by Gulder (1998). Soot formation is described as the process of hydrocarbon fuel undergoing pyrolysis or partial oxidation during combustion to form small hydrocarbon radicals from which acetylene compounds are formed, Fig 2. Large aromatic ring compounds coagulate and hypothesized as the mechanism forming the primary soot particles. Electron microscopy observations indicate that the smallest of these particles is approximately 1.5 nm in diameter. The primary particles then increase in size through a surface condensation of molecules from the gas phase, which results in surface growth. What is referred to as soot particle size is generally the coagulation of the primary particles into larger aggregates.

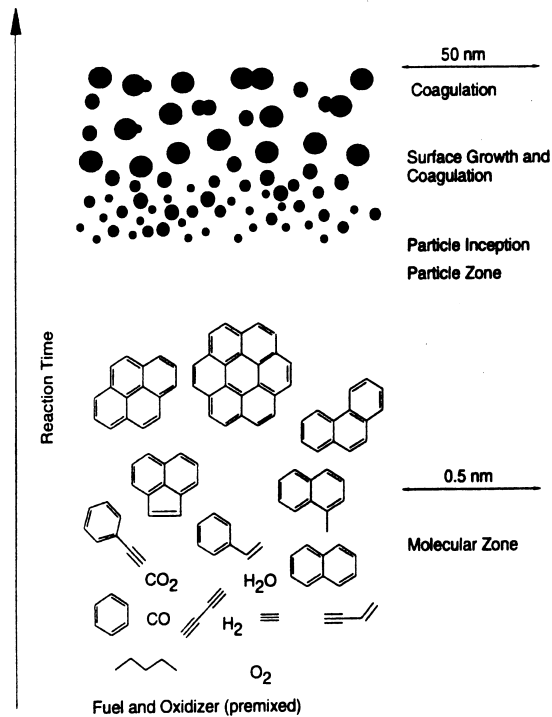


Figure 2. Schematic representation of the formation of soot for a premixed combustion condition (from H. Bockhorn (Ed), 1994 Soot Formation in Combustion, Springer-Verlag, Berlin))

A useful summary of the soot morphology and optical properties including a discussion of the Rayleigh-Debye-Gans (RDG) light scattering model and the aggregation of soot may be found in Faeth and Koylu (1995). They recognized that soot consists of nearly spherical primary particles having diameters generally less than 60 nm, which agglomerate into open structured aggregates. These aggregates grow to a wide range of sizes with the largest of the aggregates containing thousands of primary particles resulting in soot aggregate sizes of several microns in equivalent diameter. They also review the scattering models of polydisperse fractal aggregates (PFA) using the RDG approximations. An important observation regarding the formation of the soot aggregates is that the primary particles of soot tend to be somewhat merged rather than touching at points indicating subsequent soot growth after aggregation. This indicates that the soot aggregation occurred in situ and not due to the sampling process. The open structure of the soot aggregates led to the conclusion that they cannot be modeled as equivalent spherical objects. This observation was made by Snelling et al. (1997) in which they concluded that the equivalent sphere approach was faulty and that the soot particles need to be modeled as agglomerates of N_p primary particles of diameter d_p that are just touching. Faeth and Koylu point out that soot has the physical properties of carbon blacks but with significant porosity and the existence of hollow cenospheres. Soot from some internal combustion engines may also contain significant levels of volatile matter.

The primary particles of soot at given flame conditions have been recognized by a number of authors as being nearly monodisperse. The size of the primary particles varies with flame conditions and the fuel type with the largest particles being associated with the heavily sooting fuels. The aggregate particle sizes, unlike the primary particles, vary over a large range with relatively broad size distributions. When using the RDG model, the major assumptions made noted by Faeth and Koylu concerning the soot physical properties as follows: the primary particles are spherical with monodisperse diameter distributions, primary particles just touch each other, they are homogeneous with uniform refractive index, the aggregate size distributions follow a log normal distribution, and the aggregates behave as mass fractal-like objects. The investigations of Faeth and Koylu showed that the RDG-PFA theory for soot required further information on the uniformity of the primary particle physical properties, variations of the fractal properties, and the refractive indices as a function of the fuel type and flame condition.

Tien and Lee (1982), Viskanta and Menguc (1987), and Chang and Charalampopoulos (1990) have reviewed the refractive index of soot. The determinations were made by *ex situ* reflection coefficient measurements using compressed soot samples collected from flames. These methods were questionable considering the effects of the sampling and compression as well as the effects of surface roughness and voids on the reflectivity of the soot. More recently, the *in situ* measurements of extinction and light scattering by soot within both nonpremixed and premixed flames has been used to infer the refractive index. These extinction and light scattering measurements require additional information if the soot refractive index is to be acquired. Given all of the uncertainties in these methods, it is understandable that there remain significant differences in the existing measurements of the soot refractive indices. If additional measurements in the published literature were considered, the results would show a wide spread in the results indicating that the information is still inadequate for the proper characterization of soot using the light scattering and extinction approach. Faeth and Koylu recognize that it will be difficult to resolve the other issues with the light scattering approximations until a reliable method is devised for characterizing the soot refractive indices and it is this issue that merits the highest priority for future research.

Koylu (1996) found that by using the proper particle refractive indices and the RDG/PFA approach, the aggregate parameters (particle volume fraction, fractal dimension, primary particle diameter, particle number density, and aggregate size distribution) can be obtained with reasonable reliability and accuracy as determined by comparisons to thermophoretic sampling and transmission electron microscope (TS/TEM) observations. He also concluded that the soot emissivities were underestimated when using the Rayleigh analysis due to the uncertainties in the soot refractive indices at infrared wavelengths.

3. Laser-Induced Incandescence (LII)

While working with the CARS method, Eckbreth (1977) was troubled by the presence of soot particles that produced laser-modulated incandescence, which could overwhelm the signals desired in the Raman measurements. He was able to relate the time dependence of this interference to laser heating, heat transfer to the medium, particle vaporization, and indirectly to the particle size. Melton (1984) performed numerical calculations to investigate the possibility of developing a soot diagnostic based on this laser heating of particles. He concluded that it might be possible to obtain the particle temperature, soot primary particle size distribution parameters, and relative soot volume fraction. The preliminary experiments were not conclusive. Dasch (1984) modeled the vaporization of small soot particles and conducted experiments demonstrating the method. Since that time, a number of research teams have investigated the method with varying degrees of success (Dec, et al. (1991), Vander Wal and Weiland (1994), Quay, et al. (1994), Bengtsson and Alden (1995), Will, et al. (1995), Mewes and Seitzman (1997), and Snelling et al. (1997). Dec, et al. used the incandescence method to visualize the soot production inside a diesel engine.

Relative soot volume fraction measurements, which are important to the study of, soot formation, combustion radiation and heat transfer, and for monitoring combustion generated particulate may be measured using LII. Currently, an additional means for measuring the absolute soot volume fraction such as line-of-sight extinction or a calibration source is needed to relate the relative values to the absolute concentration. Santoro and his co-workers (Quay, et al. 1994) obtained spatially resolved soot volume fraction measurements using a combination of light scattering/extinction techniques on a sooting laboratory flame. They were able to use combined light scattering and LII to obtain spatially resolved number concentrations and particle sizes. When using LII, the soot particles, which are strong absorbers of radiation, are heated by a short duration laser light pulse to approximately 4,000 to 5,000 °K to produce incandescence. Laser fluence of 0.35 J/cm² is sufficient to heat the particles to this temperature. The resulting incandescence is blue-shifted relative to the normal soot radiation because of the high soot temperatures. This signal is easily detected using PMT's with filters. The method can be used to obtain quasi-point or planar measurements of the soot volume fraction.

Ni, et al. (1995) pointed out that with a variation in laser fluence, the decay constant of the LII signal varies significantly. Their conclusion was that such a dramatic effect could not be explained by reduction in the soot particle size alone and that it may be due to significant changes in the soot morphology. However, the authors were only looking at delay times up to approximately 100 ns where vaporization is expected to be the dominant heat loss mechanism. In addition, the experiments included fluence values where vaporization temperatures were not reached.

A number of papers on the subject were written by Vander Wal and his colleagues (Vander Wal and Weiland, 1994, Vander Wal and Dietrich, 1995, Vander Wal et al. 1996, Vander Wal, 1997, Vander Wal et al. 1998, Vander Wal,

1998, and Vander Wal and Jensen, 1998). Vander Wal and Weiland (1994) recognized that the LII signal is unaffected by the elastic light scattering contributions which affect the light absorption measurements of large soot aggregates and the uncertainties in the complex refractive indices. For soot aggregates that may be as large as 10mm, the light extinction measurements must be corrected for the light lost by scattering. They pointed out that the LII signal depends upon 1) the excitation and detection wavelengths, 2) the excitation intensity, 3) detection timing and duration, and 4) the soot volume fraction. These dependencies must be studied and characterized if a reliable diagnostic is to be developed. The authors also recognize the need for a delay between the laser pulse and the signal collection gate to allow any molecular and photofragment emissions to decay either through quenching or radiative processes. Their attempts to fit the measured emission spectra to a single temperature back-body curve did not meet with success. Later work by Snelling et al. (private communications) served to explain these differences and these results will be provided in the final report. Vander Wal and Weiland also recognized that the soot particle size affects the heating and the cooling rates of the soot particles and hence their temperature and emissions. Particle aggregates that are too large to be in the Rayleigh regime are predicted to heat at different rates since the absorption cross section is dependent upon the surface area. Soot of different sizes will have different surface-to-volume ratios and hence, will cool at different rates. They state that the observed emission curve during and after laser light excitation will be a combination of several black body radiation-time curves at different temperatures weighted by the particle size distribution and convolved with the wavelength. Subsequent studies by others show that the LII signal is dependent upon the size of the primary particles, which are nearly monodisperse. Their experiments showed that the temporal nature of the LII signal was rather independent of the soot-particle history at different measurement heights in the flame. Line-of-sight extinction was used to obtain the absolute measurements of the soot volume fraction. They found that the dependence of the LII signal was relatively insensitive the laser intensity used in the measurements as long as saturation is reached when utilizing a 50 ns signal collection gate. It will be shown by Snelling et al. that there is more to this observation and that the laser fluence used is an important parameter. They recommend using a collection over as wide a spectral range and temporal bandpass as possible.

Vander Wal, et al. 1996 used gravimetrically determined soot volume fractions to calibrate the LII method and demonstrate the linearity of the LII calibration over an range of volume fractions from 0.078 to 1.1 ppm. This approach had the advantage over line-of-sight extinction in that all of the uncertainties of the refractive indices are removed. Both point and planar measurements were evaluated to examine any possible morphology bias in the LII signal. The authors suggest that the gravimetric sampling approach offers a calibration means for a wide range of soot volume fraction conditions. Given the accurate absolute calibration means, the LII method can provide information with high temporal and spatial resolution.

An investigation of the effects of the rapid heating of soot which has the potential of producing chemical and physical changes in the soot and raises questions as to how the LII signal may be affected by these changes was conducted by Vander Wal, 1995. TEM micrographs were obtained of soot samples for soot not irradiated by the laser and for soot collected using thermophoretic sampling after irradiation with the pulsed laser. The latter showed unusual shell structures. For some of the soot particles, apparent small structures within the shell were observed whereas other particles appeared to have voids or porous material in the inner core. Adjacent particles were observed to show a more normal morphology. They demonstrated with the use of X-ray analysis that the shell structures were soot not some contaminant material. The surmise that since preferential vaporization/volatilization of the interior of the soot particles occurs during the pyrolysis of coal and heavy fuel oils, it may also account for the present observations. These changes in the soot morphology could alter the heat transfer characteristics of the heated soot since the voids inside the spheres will reduce their mass and allow the particle to cool more rapidly than equivalent solid particles. They also hypothesize that it may be the PAH's that are driven out of the soot leaving a more representative measure of the carbon soot volume fraction.

Several studies have been conducted to determine whether the primary soot particle size may be determined using LII. The theory indicates that the decay of the signal after excitation may be related to the primary particle size since the cooling of the particles is primarily through conduction and convection which is dependent on the surface area. Vander Wal, et al. (1998), proposed two methods based on a theoretical model for obtaining the particle size information. One method used the ratio of the signal intensity at two wavelengths integrated over the same time delay and duration after the laser pulse. The second method used the same averaged temporal curve at a single detection wavelength with a gate ratio formed at two different delays after the laser pulse. The results were compared to thermophoretic sampling with subsequent TEM microscopy observations. Concerns were expressed over the fact that in regions of the flame, the aggregates become larger and more dense and compact. Changes in the

structure can be expected to cause a decrease in the cooling rate of the individual primary particles. Nonetheless, good agreement was achieved in certain regions above the burner face.

Vander Wal and Jensen, 1998 investigated the effects of laser fluence upon the LII signal and the potential for the heating to change the soot morphology and properties. The laser light fluence used is generally established empirically by observing the LII signal which increases rapidly, then becomes nearly constant, and then decreases with increasing laser fluence. The Light fluence is chosen for the plateau region observed from the signal. The authors indicate that several physical processes are hidden in this signal behavior. Their data and TEM images suggest that dramatic changes are taking place in the soot morphology during laser light heating. The temporal decay rate of the signal increases while the peak intensity increases with increase in laser fluence. The outcome integrated over the detector gate time is an nearly constant signal for a range of fluence. The laser-heated particles have a higher rate of cooling since the surface area to solid volume ratio is greater for hollow spheres than for solid particles. At laser light fluence greater than 0.5 J/cm^2 the peak signal intensity was observed to decrease since the temporal decay rate of the incandescence continues to increase due to the morphology change in the soot and significant increase in the soot vaporization rate takes place. Another factor that was not discussed is the effect of the Gaussian beam intensity profile. Even while the light fluence at the center of the beam is causing significant soot vaporization, a range of soot temperatures is generated by the lower light intensities on the wings of the Gaussian beam.

The dependence of the LII signal on the aggregate morphology, primary particle size and initial particle temperature as well as the beam intensity profile and excitation wavelength need further attention. For example, the absorption constant for soot at 1064 nm is less than half that at 532 nm with the scaling at approximately $1/\lambda$. After the observation that the soot particles may form hollow spheres due to laser beam heating, the authors designed their experiments to further examine these effects on the LII signals. They used a two-pulse technique with each 10 ns pulse duration separated by 10 μ s. with one laser pulse producing the changes to the soot particles and the second pulse was used to interrogate the same particles using the LII approach. Comparisons of the signals made with one laser pulse were used to determine if the laser heating affected the morphology and hence, was significant to the results obtained. The laser light heated and unheated and soot was sampled using thermophoretic sampling and observed with a TEM. Vander Wal and Jensen found that for one pulse designated P_1 , fluence from 0.36 to 0.55 J/cm^2 the relative signal intensities in the annular region of the flame were relatively constant. Profiles generated by the second pulse, P_2 at lower fluence of 0.18 to 0.36 J/cm^2 resulted in similar intensities. Fluence of 0.55 J/cm^2 produced a significant decrease in the LII intensity, which was believed to be a result of the changes in the optical properties of the soot as well as mass loss, caused by the P_1 laser pulse. The authors found good similarity in the profiles produced by the P_1 and P_2 strategies showing the robustness of the LII method. Although different absolute intensities were produced with the P_1 and P_2 , the normalization of the signal profiles showed self-similarity. The profiles at 40 mm above the burner showed significant dissimilarities for the P_1 and P_2 cases. They surmised that a possible reason may be the size-dependent heating and cooling effects related to the primary particle and aggregate size, local temperature, and vaporization or altered soot morphology. The authors also note that the sphere surface to volume ratio scales as $1/r$ where r is the radius of the sphere. So smaller particles will necessarily cool faster than larger particles. Another explanation offered was that the soot particles became increasingly "graphitized" with increasing laser fluence wherein the particles develop a shell structure. The process increases the effective surface area relative to the solid volume. In addition, the primary particles were observed to within the aggregates became more highly fused together and at sufficient laser light fluence, merged to produce a single hollow particle.

The authors evaluated their LII results using extinction measurements. Over a range of laser light fluence from 0.9 to 0.73 J/cm^2 they obtained good agreement to within 5% of the correct value at 20 mm above the burner. The agreement held over a wide range of soot particle size, morphology, and oxidation state and growth of the soot. They concluded that the LII signals are strongly dependent on the excitation laser light fluence. The laser light fluence was believed to cause significant changes in the physical structure in both soot primary particles and aggregates. Using the double pulsed approach, it was shown that the soot heated by a prior laser pulse confirmed the change in the soot due to varying excitation laser light fluence. Despite the changes, the LII radial intensity profiles for a laminar diffusion flame showed self-similarity.

Filippov et al. (1999) investigated the possibility of sizing very small particles using the LII approach. Their work was unique in that they looked at ultrafine carbon, silver and TiN particles as well as aerosol particles dispersed in

air. The carbon (graphite) particles, which have properties very close to soot with small primary particles and large aggregates, were produced with a commercial spark generator. Silver particles were produced using a condensation process. The TiN aerosol was dispersed by an expansion wave aerosol generator. Similar to others, they recognized that the particle cooling is strongly size-dependent so this information can be used to estimate the primary particle size and possible, the fused aggregates. The authors recognized the difficulties in dealing with polydisperse particles that are illuminated by a laser pulse with spatially varying intensity in the sample volume. Heating and cooling of the individual particles is determined by the local laser beam pulse light intensity which is not uniform over the measurement volume, the particle size, and the particle material properties. The authors also surmised that the larger aggregates may be partially disintegrated by the laser pulse. The presented evidence of this by examining the raw graphite aerosol. With increasing laser pulse energy, the size distributions were noted to become narrower and shifted towards smaller particle sizes. At high laser pulse energies (300 mJ), the size decreased to that of the primary particle size of approximately 5 nm in diameter. The particle sizes obtained for low pulse energy were comparable to the sizes obtained with the mobility size distribution for raw graphite particles. UV wavelength at 335 nm generated from the third harmonic was used for the LII measurements of the silver particles. The results were compared to the results from a Differential Mobility Analyzer (DMA). The TEM images were also used to derive the size statistics. The agreement between the LII measurements and the TEM and DMA analysis was quite good. Filippov et al. concluded that the lower sensitivity limit of the LII method was below 10^3 particles per cm^{-3} . This implies that the method can be used for atmospheric particle studies. They also suggest that the method could be used for quality control in processes such as ceramic particle production in chemical reactors.

Wainner, et al. (1997) investigated the LII method for obtaining soot volume fraction and particle size using a “soot generator” which dispersed carbon black particles in the form of an aerosol. This eliminated any effects of local reaction and the unknown ambient gas temperature. Using a range of dilutions for the aerosol, a range of soot concentrations spanning 4 orders of magnitude was tested. They found acceptable linearity and accuracy in the soot volume fraction over this large dynamic range. They found the particle size dependence to scale as $d^{3.2}$, which may well be considered as d^3 , or proportional to the particle volume. They also showed a non-monotonic size dependence with the calibration constant increasing for small particles, reaching a peak and then decreasing for larger sizes. In a subsequent paper in which they considered such parameters as gas temperature, particle size, laser fluence, and soot composition and morphology, Wainner and Seitzman, (1999) showed some considerable difficulty in obtaining plausible results. They tried two approaches for obtaining the particle size, one based on the predicted change in maximum temperature reached by different sized particles and the other based on the variation in the rate of conductive cooling with particle size. With increased laser light fluence, the temperature of the particle increases, as does the vaporization rate until a balance is obtained. When the laser light pulse ends, the vaporization rate falls and the dominant cooling becomes conductive to the surrounding gas. The energy loss due to the mechanisms of conduction and evaporation are expected to vary as d^2 . Their model and that of others predicts that the particles of different sizes will reach different maximum temperatures and cool at different rates. They indicate that the LII signals produced during the conductive cooling should depend on the particle size, temperature just after the vaporization period, the surrounding gas temperature, and the conductive cooling rate. They also recognize that the cooling mechanisms should be dependent upon the primary particle size, especially at longer delays wherein the gas temperature could become a factor.

A recent paper by McManus, et al. (1998) suggests the ability to make both soot volume fraction and particle size distributions in combustion flows. The authors pose the coupled differential equations describing the LII heat balance for a given particle size as:

$$V_p \rho_s c_s dT / dt = Q_{\text{absorption}} + Q_{\text{conduction}} + Q_{\text{vaporization}} + Q_{\text{radiation}} + Q_{\text{thermionic}} \quad (1)$$

$$\rho_s dr / dt = -\rho_v U_v \quad (2)$$

where V_p is the volume of the particle, r_s and c_s are the density and specific heat of the soot, Q quantities represent the heat gain or loss in W/particle by the various mechanisms, and ρ_v and U_v are the density and the velocity of the vaporized carbon. The equation may be numerically integrated. However, the authors provide several caveats or warn of potential sources of uncertainty such as the formulation of the heat loss terms, the effect of the radial intensity profile of the laser beam, thermal response of the small particles to the high energy laser beam, the values

of some of the thermodynamic parameters for soot and its vapor, and the physics associated with the non-spherical particles. The authors also provide the expression for heat input by absorption of the laser beam as:

$$Q_{absorption}(r, \lambda) = \pi r^2 Q_a(r, \lambda) = (\rho_s N_0 / M) V_p(r) \sigma_a(r, \lambda) I_o(\lambda) \quad (3)$$

where Q_a is the Mie absorption efficiency for a given light wavelength and particle radius. The thermal conduction between the soot and the surrounding gas is described by spherical free-molecular heat transfer. Since the soot particles are generally less than 100 nm in diameter and the mean free molecular path is approximately 400 to 600 nm, the Knudsen number $Kn > 1$. The authors recognize that the radiative heat transfer is not significant as was indicated by Melton (1984) previously.

McManus et al. also examined the effect of the laser intensity (more accurately, the light fluence) on the LII signal. As others, they found that the LII signal increases with increasing laser fluence until a plateau in the LII signal is reached. This is believed to be due to the soot having reached the vaporization temperature of approximately 4500°K. They investigated the signal sensitivity on the soot properties at various heights in the flame. The soot volume fraction and primary and aggregate particle sizes will change by a factor of five along the axis of the flame. The observed results at three axial locations showed similar saturation curves with laser energy. Their observation led them to believe that the saturation process causing the plateau in the LII intensity was only weakly dependent upon the local soot properties. At high laser light intensities, they suggested that the soot properties including the particle mass, structure of the aggregates, and optical properties such as the complex refractive index were modified during the heating, which resulted in a decrease in the LII signal before the end of the light pulse.

Soot primary particle size measurements were also attempted by McManus, et al. using the LII method and SEM micrographs for comparison. Two flames were used with equivalence ratios of 1.5 and 1.8. A set gate width was used to measure the incandescence signal at delays from 0 to 1.1 ns from the trailing edge of the laser light pulse. The cooling rates predicted using the heat transfer model were used to obtain primary particle size from the LII signal decay rate. The model predicted particles in the size range of 30 and 40 nm in diameter for the equivalence ratios of 1.5 and 1.8. The SEM micrographs showed primary particle sizes to be approximately 20 and 40 nm in diameter. At higher particle temperatures, they found a discrepancy in the vaporization-dominated regime. The authors conclude that there may be a change in the soot properties due to excessive heating.

In a paper by Appel, et al. (1994), LII measurements were made for a laminar premixed sooting flame with the goal of evaluating the influence of particle properties on the LII signals. The experimentally obtained LII signals were compared with the theoretical calculations of the LII signals. The LII signals were detected with a gate-delay time of 90 ns and a gate width of 250 ns. They found that detection at different wavelengths did not significantly influence the LII signal profiles. Comparisons between the soot volume fractions obtained from the measured and calculated LII signals were made after calibration with the corresponding soot volume fraction obtained by extinction measurements. They found that the soot volume fractions obtained via the calculations were approximately a factor of two larger than the values obtained experimentally. The authors surmised that the discrepancies could be due to change in the refractive indices. However, they found that changes in the refractive index influenced the absorption efficiency, the mean particle size, and the number density in a manner such that the effects were approximately compensated. They then explored the effects of a change in shape of the particles from spheres to ellipsoids with varying eccentricity. It was found that a variation in the particle shape had a strong influence on the temperature and the spectral response which seriously affect the LII signals and hence, the corresponding soot volume fraction. Even a small variation in the particle shape was recognized to produce large deviations between the calculated and the measured LII signals.

Mewes and Seitzman (1997) attempted to obtain particle size information using a pyrometric technique involving the ratio of LII signals obtained at two wavelengths (400 and 700 nm). This method uses the temperature decay as a function of particle size. The method was claimed to be relatively independent of the flame temperature but unfortunately, was also relatively independent of the particle size. At longer decay times, the temperature decay becomes more sensitive to particle size but it is also more dependent upon the generally unknown ambient temperature in the flame. The laser fluence used was much higher than that used by others so a good deal of vaporization could be expected. Additional problems arise from the fact that the two-wavelength method requires knowledge of the spectral variation of the refractive index of soot, the wavelength dependence of the absorption, and

the detector spectral sensitivity. An accurate model for the soot temperature at any given time after laser light excitation is also required.

Will et al. (1998) had the goal of providing an analysis of the factors affecting the performance of the LII method for particle sizing. An attempt is made to show how the ratio of the LII signal at two delay times can be used to determine the primary particle size. They begin with the recognition that the LII signal is dependent upon the particle size and temperature with the expectation that the size will change due to vaporization. The assumption is made that the primary particles are spherical and form aggregates of varying and unknown size. Absorption of light and emission of radiation is assumed to be from independent primary particles since the soot aggregates have been observed to be loosely structured aggregates with fractal dimensions in the range of 1.5 to 1.8. The authors numerically integrate the power balance equation to show that the vaporization heat loss is dominant to approximately 100 ns after excitation and then the conduction mechanism is dominant and determines the temperature decay rate, figure 3. When setting up the relationship for predicting the LII signal, the assumptions were made that the particles were nearly monodisperse and had a uniform temperature over the sample volume. This latter assumption is not met due to the Gaussian beam intensity profile. They claim that the overall effect on the particle sizing will be negligible. It was also pointed out that the knowing the laser beam intensity profile, they could calculate the integral signal from the various regions of illumination. The issue of the signal-to-noise ratio (SNR) was considered and it was recognized that for time-averaged measurements wherein an ensemble of measurements could be added together, good SNR can be achieved. In turbulent flows where single shot measurements are required, the SNR can be a problem especially if a high spatial resolution is also required. If a larger sample volume is used, stronger signals can be obtained.

The authors argue that the laser Gaussian intensity profile does not present a significant problem since the error in the determination of the particle size is almost linearly dependent on the deviation from the nominal laser irradiance over a fairly wide range. They state that the size determined from the mean value that is due to larger and smaller values of irradiance nearly cancel each other. Hence, the results for a Gaussian profile beam should be the same as that for an equivalent rectangular intensity profile. They do recognize that there is a residual effect due to the fact that the intensity on the wings of the Gaussian beam is insufficient to bring the particles to the vaporization temperature but claim that there is little contribution to the signal due to the lower temperatures. In general, we do not agree with this latter assumption and the point will be addressed further in a later section. The authors also comment on the effect of the refractive index on the measurements. They select a value of $m = 1.57 - 0.56i$ which is not actually based on any measurement. The imaginary component (which determines the absorption) is most important and they indicate that even for a range from 0.37 to 0.8, the error in the size determination is only +/-10% from if the assumed value of 0.56 is used.

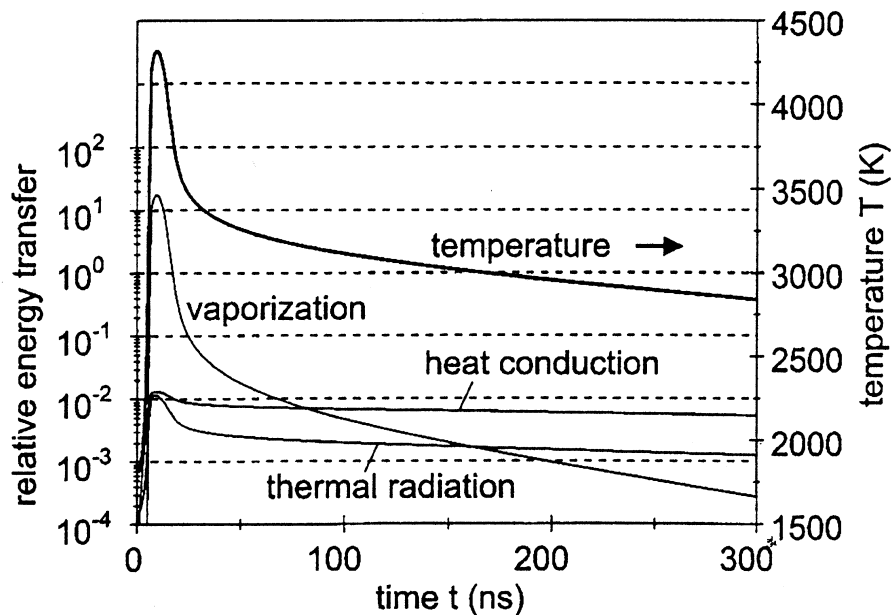


Figure 3. Plot showing the theoretical description of the relative magnitudes of the heat loss mechanisms for laser light heated soot particles (from Will, et al, 1998).

An argument is made by Will et al. (1998) regarding the effects of the particle vaporization to address the fact that the heat of vaporization and the vaporization temperature are subject to large uncertainties. They indicate that these parameters do not affect the cooling mechanisms for the LII time scales used but determine only the shrinkage of the soot particles. This small shrinkage was accounted for in the model and if an error was made it was expected to be small since a small change in size is associated with a high amount of energy transferred. If the energy transferred due to vaporization were modeled incorrectly, only a small error in measured size would result. The authors claim that since the heat conduction is proportional to the difference between the particle and the surrounding gas temperature, there must be a significant influence of the gas temperature, T_0 on the accuracy of the particle size determination. The conclusion would be to use earlier detection times but in this region, the size dependence requires adequate separation in detection times for reasonable size dependence.

Some concern was expressed regarding the shape and contact area of touching neighboring particles. The shape of the primary particles was shown previously to have a significant effect on the signals. It was also recognized that the particle heat conduction surface is reduced by approximately 10% from that of an isolated sphere due to touching neighboring particles. The heat loss will also depend on where the sphere is within the aggregate. Concern was also expressed about the mutual interference of the heat loss of individual particles. The authors showed rather impressive results for particle size profiles across the flame along with the relative independence of the size information on the laser fluence, figure 4 and detection wavelength, figure 5. Since the particle size measurements are obtained from the ratio of signals, the technique is relatively insensitive to interfering effects such as signal absorption. The authors

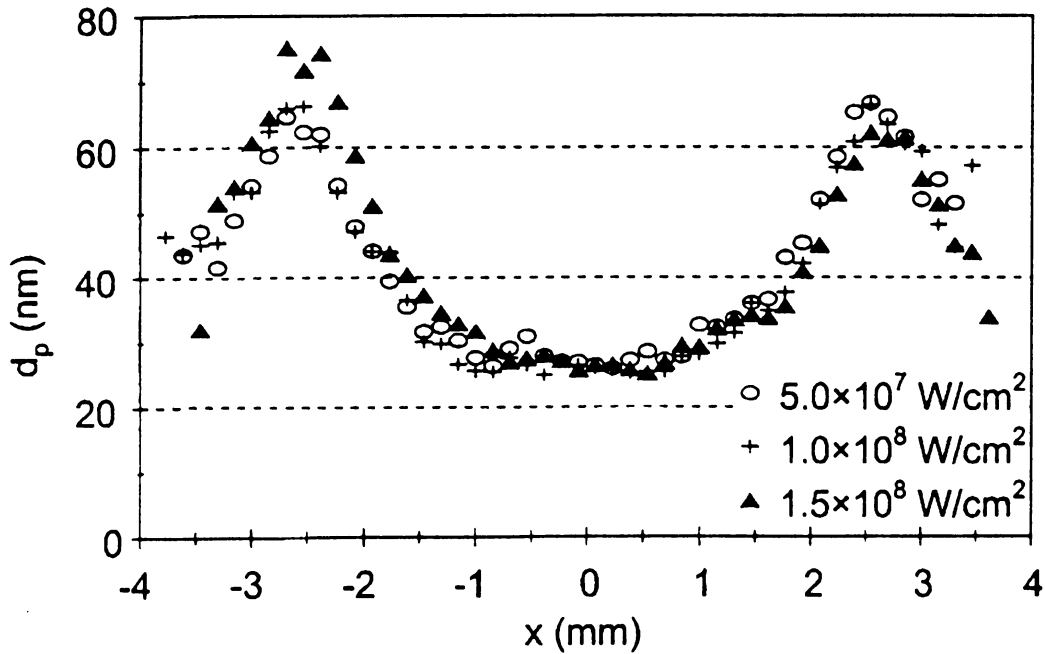


Figure 4 Radial profiles at 20 mm above the burner face of the primary soot particles sizes for various laser light irradiance values (from Will et al., Applied Optics,1998).

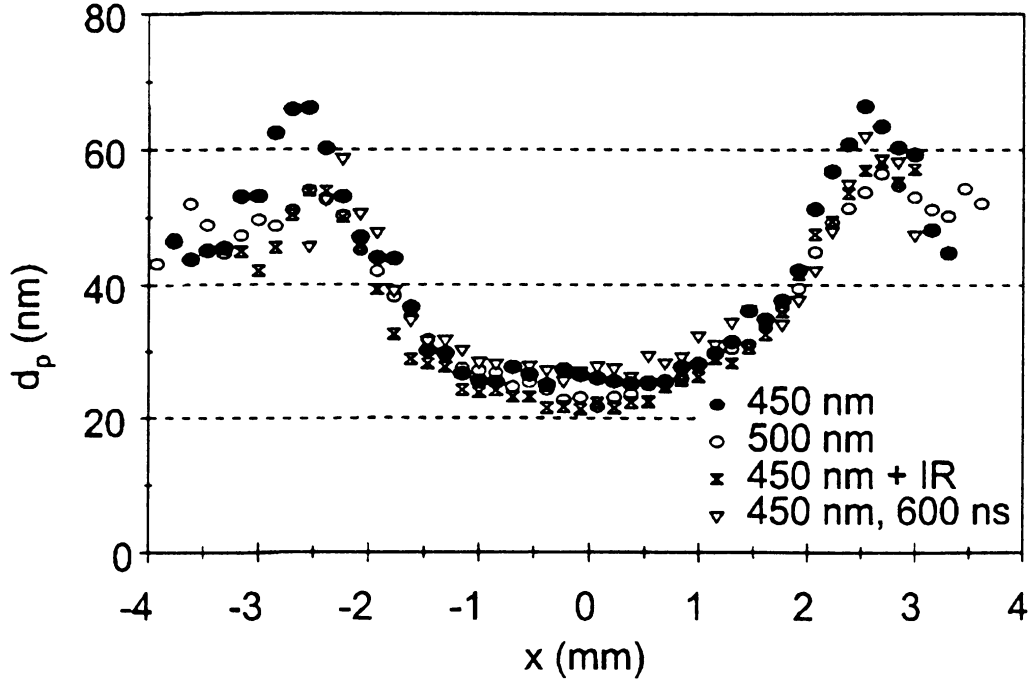


Figure 5 Radial profiles at 20 mm above the burner face of the soot primary particle size for different spectral filters on the detectors (from Will et al., Applied Optics, 1998).

claimed good consistent qualitative agreement but admitted that improvements to the quantitative measurements will require extensive work on both the models of heat transfer and the input data.

Description of Method

Significant work has been devoted to the theoretical modeling of the transient soot heating and cooling characteristics going back to the work of Melton, (1984) and others. The analysis outlined follows the work of Snelling, et al. (1997) who improved upon the analyses of Hofeldt (1993). Soot particles are described as aggregates of N_p soot primary particles of diameter d_p , as suggested by Dobbins and Megaridis, (1987) that are just touching. The aggregate volume is the sum of the volumes of the individual primary particles and since the primary particles are considered to be of nearly uniform size, the volume may be stated as $N_p d_p^3$ and $D_{es} = N_p^{1/3} N_p$. The heat transfer equation for the energy balance for a transient heated (by 10 ns laser light pulse) soot particle is given as

$$C_a q - \frac{2k_a(T - T_0)\pi N_p d_p^3}{(D_{ES} + G\lambda_l)} + \frac{H_v}{M_v} \frac{dM}{dt} + q_{rad} - \frac{\pi N_p d_p^3}{6} \rho_s c_s \frac{dT}{dt} = 0 \quad (1)$$

The first term represents the absorbed laser light energy by the soot aggregate where q is a function describing the laser intensity in W/cm^2 and C_a is the soot absorption cross section. The last term is the laser heating where ρ_s is the soot density (kg/m^3) and c_s is the specific heat of carbon. Thus, in the present analysis, the aggregates are taken as an agglomerate of just touching primary spheres of nearly monodisperse diameter d_p that are well within the Rayleigh limit. The absorption coefficient C_a for the aggregate is now assumed to be that of the N_p primary particles given as

$$C_a = N_p C_p = N_p \frac{\pi^2 d_p^3 E(m)}{\lambda} \quad (2)$$

where the complex refractive index is given as $m = n + ik$ and

$$E(m) = -\text{Im}[(m^2 - 1) / (m^2 + 2)] \quad (3)$$

and so

$$E(m) = \frac{6nk}{(n^2 - k^2 + 2)^2 + 4n^2k^2} \quad (4)$$

For a wavelength of 1064 nm and a refractive index obtained from the dispersion relationship from Dalzell and Sarofim is $m = 1.63 + 0.7i$ and $E(m) = 0.30$ while at 532 nm, $m = 1.59 + 0.58i$ and $E(m) = 0.26$.

The second term describes the heat transfer to the surrounding medium, specified in terms of the aggregates of primary particles. In the expression, G is a geometry dependent heat transfer coefficient specified as

$$G = \frac{8f}{\alpha(\gamma + 1)} \quad (5)$$

where f is the Eucken factor equal to $5/2$ for monatomic species, α is the accommodation coefficient normally assumed to be ~ 0.9 , $\gamma = c_p/c_v$ ($=1.4$ for air) is the ratio of specific heat coefficients. Snelling, et al. (1997) have recently discovered the work of Leroy, et al. (1997) in which they made measurements indicating that the accommodation coefficient of nitrogen on solid graphite in the temperature range of 300 to 1,000 °K gave a value of 0.26. Snelling et al. found that the analysis with an accommodation coefficient of 0.9 incorrectly predicted the very fast decay in the LII signal whereas the value of 0.26 gave good agreement with the experiment.

The expression describes the heat transfer to the surrounding medium in the case of the transition regime between free molecular and a continuum. However, the soot aggregates are generally smaller than the molecular mean free path length in the typical flame environments. That is, the Knudsen number, $K_n = l/D_{es}$ is much greater than 1 and hence, the heat transfer coefficient is independent of the particle size. It should also be noted that in the denominator, $Gl \gg D_{es}$ so the dependence of the soot particle diameter becomes insignificant in this term.

The third term in the expression describes the loss of heat from the particle due to evaporation of the carbon. The rate of mass loss is given by the analysis of Hofeldt (1993) assuming that the particle surface is essentially stationary and that the vapor is lost by diffusion is given as

$$\frac{dM}{dt} = \frac{\rho_s}{2} \pi d_p^2 \frac{dd_p}{dt} = - \frac{N_p \pi d_p^2 N_v M_v}{N_{AV}} \quad (6)$$

where N_v is the molecular flux of evaporating carbon vapor for the free molecular condition ($K_n \gg 1$), M_v is the soot vapor molecular weight and N_{AV} is Avogadro's number.

The fourth term describes the radiative heat loss by N_p primary particles given as

$$q_{rad} = 4\pi^2 N_p \sigma_{SB} T^4 \left(\frac{E(m)}{\lambda} \right)_{532} \quad (7)$$

where the parenthetical expression is evaluated at the wavelength of interest. Compared to the other heat loss mechanisms, the heat loss due to radiation is insignificant.

The last term which is

$$\frac{\pi N_p d_p^3}{6} \rho_s c_s \frac{dT}{dt}$$

describes the particle heating where ρ_s is the soot density and c_s is the specific heat of carbon.

The heat transfer equations derived represent a set of two coupled differential equations that needed to be solved numerically for the soot particle diameter (dd_p/dt) and soot temperature, dT/dt . Rearranging the heat transfer energy balance equations and making the appropriate substitutions, the relationships for a single primary soot particle are expressed as

$$\frac{dd_p}{dt} = - \frac{2f_{mw}(T)}{\rho_s RT} \frac{f_{vp}(T)}{\frac{1}{\beta} \left(\frac{2\pi f_{mw}(T)}{RT} \right)^{1/2} + \frac{d_p^{1/3} N_p}{2D_{AB}}} \quad (8)$$

where $f_{vp}(T)$ is an empirical factor for the vapor pressure and $f_{mw}(T)$ for the molecular weight, and D_{AB} is the inter-diffusion coefficient for soot vapor into the surrounding gas. Snelling et al. solved the equations numerically to obtain an expression for the time history of the LII signal as

$$I(t, \lambda) = \frac{2\pi c^2 h}{\lambda^5} \left[e^{\frac{-hc}{\lambda kT(t)}} - 1 \right]^{-1} \pi N_p d_p^2 K_{ap}(\lambda) \Delta \lambda \quad (9)$$

where

$$K_{ap} = \frac{4\pi d_p E(m)}{\lambda} \quad (10)$$

and h is the convection coefficient. The equation shows the dependence of the LII signal on the primary particle diameter, d_p , the particle temperature, $T(t)$, the emission wavelength, λ , and the thermal conductivity, k .

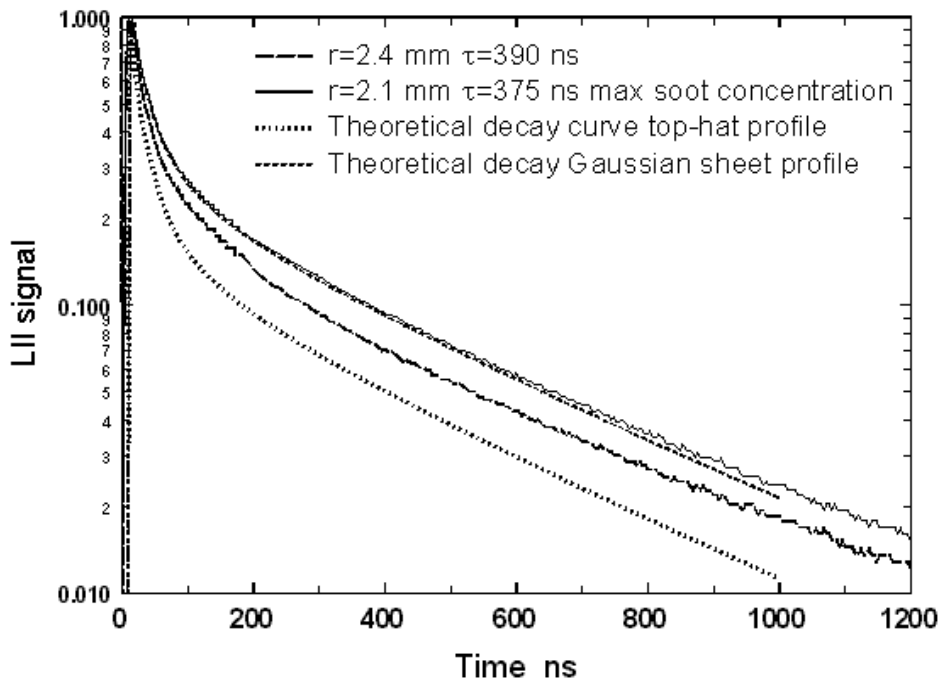
Results:

Snelling, et al. recognized that the Gaussian beam intensity profile of the laser light sheet should be accounted for in the analysis. The calculated signal intensities, $I(\lambda, t)$ must be integrated over the Gaussian range of fluence across the thickness of the laser light sheet described as

$$F(x) = F_0 \exp\left(-\frac{x^2}{w_x^2}\right) \quad (11)$$

where w_x is the $1/e^2$ half width sheet thickness and F_0 is the peak fluence in the probe volume at the center of the sheet. Although it has been argued that the fluence and hence the Gaussian beam intensity or fluence profile does not affect the results, the experimental data show this not to be true. The results indicate that the excitation curve is strongly dependent on the spatial laser intensity distribution, figure 1. Experimentally, the strong effect of the spatial laser intensity distribution on the excitation has been observed by Ni et al. (1995). A similar finding has also been demonstrated theoretically by Tait and Greenhalgh (1992, 1993) for rectangular and Gaussian laser beams. The physical reason behind this strong dependence has been discussed by Snelling et al. (1997).

Figure 1. Examples of the theoretical soot temperature decay curves compared to the recorded experimental results.



The effects of the Gaussian beam intensity profile are compared with the simple assumption of uniform beam intensity.

The LII method was evaluated using soot measurements in laminar and turbulent flames by comparing the measurements to line-of-sight light beam extinction measurements, figure 2. Using the Abel inversion, the spatial variation of the soot volume fraction was extracted from the line-of-sight extinction measurements and compared

with the approximate point measurements obtained with the LII system. With calibration, the agreement is shown to be very good. Soot volume fraction measurements were also obtained in a diesel exhaust and compared with simultaneous gravimetric results. Figure 3 shows the comparison of the LII soot volume fraction results compared with the gravimetric results. The results were in good agreement over two orders of magnitude. It was found that the gravimetric results tended to have greater uncertainty than the LII results.

In the proposed paper, details of the LII analyses will be presented to demonstrate the validity of the theoretical LII heat transfer model, the effect of the laser fluence, and the effects of the laser beam light intensity distribution. Additional results and analysis of the soot volume fraction measurements will be provided.

References:

1. Melton, L.A., (1984), "Soot Diagnostics Based on Laser Heating", Applied Optics, Vol. 23, No. 13.
2. Snelling, D.R., Smallwood, G.J., Campbell, I.G., Medlock, J.E., and Gulder, O.L., (1997), "Development and Application of Laser-Induced Incandescence (LII) as a Diagnostic for Soot Particulate Measurements", AGARD 90th Symposium of the Propulsion and Energetics Panel on Advanced Non-Intrusive Instrumentation for Propulsion Engines, October, Brussels, Belgium.
3. Hofeldt, D.L., (1993), "Real-Time Soot Concentration Measurement Technique for Engine Exhaust Streams", SAE Paper No. 930079.
4. Dobbins, R.A. and Megaridis, C.M., (1987), "Morphology of Flame-Generated Soot as Determined by Thermophoretic Sampling", Langmuir 3, 254-259.
5. Ni, T., Pinson, J.A., Gupta, S., and Santoro, R.J., 1995, "Two-dimensional Imaging of Soot Volume Fraction by the Use of Laser-induced Incandescence", Applied Optics, Vol. 23, No. 13, pp 2201-2208.
6. Tait, N. P. and Greenhalgh, D. A., 1992, "2D laser induced fluorescence imaging of parent fuel fraction in nonpremixed combustion", 24th Symp. (Int.) on Combustion, pp.1621-1628, The Combustion Institute.
7. Leroy, O., Perrin, J., Jolly, J., and Pealat, M., (1997), "Thermal Accommodation of a Gas on a Surface and Heat Transfer in CVD and PECVD Experiments", Journal of Physics D 30, 499-509.

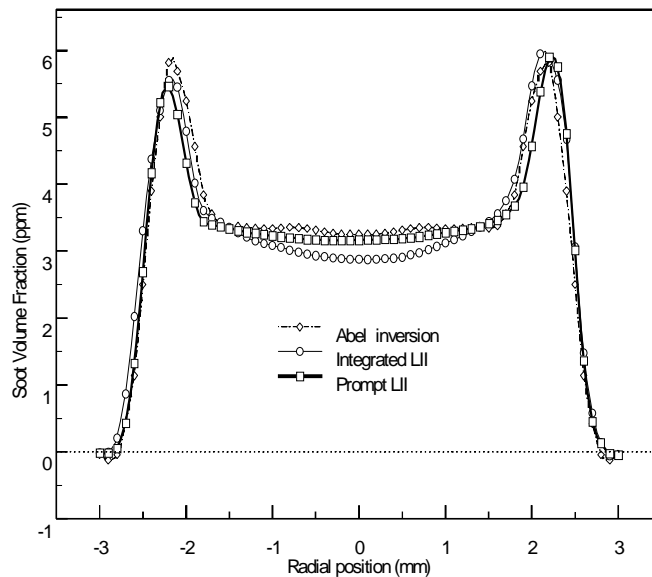


Figure 2. Volume fraction comparisons for data obtained with the LII and line-of-sight extinction measurements using the Abel inversion.

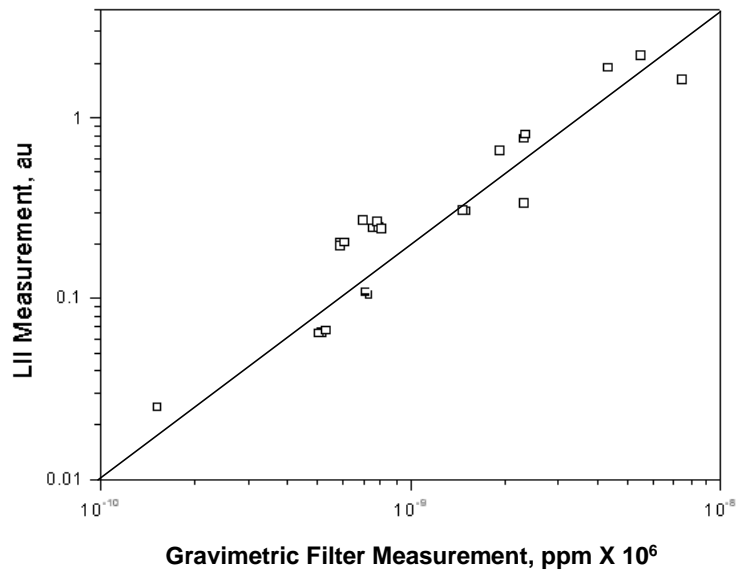


Figure 3. Comparison of the LII and filter data obtained in the exhaust of a research diesel engine.